UCRL-ID-146579

Moisture Retention Curves of Topopah Spring Tuff at Elevated Temperatures

W. Lin, R. Roberts, E. Carlberg, D. Ruddle, R. Pletcher

November 30, 2001

U.S. Department of Energy

Lawrence
Livermore
National
Laboratory

Moisture Retention Curves of Topopah Spring Tuff at Elevated Temperatures

Wunan Lin, Jeff Roberts, Eric Carlberg, Dave Ruddle, and Ron Pletcher
Lawrence Livermore National Laboratory

Introduction

Knowledge of unsaturated flow and transport in porous media is critical for understanding the movement of water and solute through the unsaturated zone. The suction potential of rock determines the imbibition of water and, therefore, the moisture retention in the matrix. That, in turn, affects the relative importance of matrix flow and fracture flow, and their interaction, because greater suction potential moves more water from fractures into the matrix and therefore retards fracture flow. The moisture content as a function of the suction potential is called a moisture retention curve or a characteristic curve. Moisture-retention data are important input for numerical models of water movement in unsaturated porous media. Also important are the effect of sample history on the moisture-retention curves and whether there is significant hysteresis between wetting and drying measurements.

The Yucca Mountain Site Characterization Project (YMP) of the U.S. Department of Energy is studying the suitability of the tuffaceous rock at Yucca Mountain, Nevada, for a potential high-level nuclear waste repository. The potential repository horizon will be in the unsaturated zone of the Topopah Spring member (densely welded) of the Paintbrush Tuff unit at Yucca Mountain. This unit is highly fractured. Therefore, transport of water within the near field of the nuclear waste package in the repository is strongly influenced by the suction potential of the repository host rocks at elevated temperatures. In a high-level nuclear waste repository, the rock mass around the waste packages will become dry because of the thermal load of the waste but will then re-wet during the cool-down period as the thermal output of the waste packages declines. Much of this process will occur at temperatures above ambient temperature. The goal of our work is to determine the importance of temperature and the wetting-drying hysteresis on the measured moisture retention curves of the densely welded tuff. For Topopah Spring tuff the suction potential is assumed to be primary due to the matric potential (See next section for explanations).

The drying (desorption) suction potential of the tuffaceous rocks at ambient temperature was measured by Peters et al. (1984), Klavetter and Peters (1987), and Flint (1998). Daily and Lin (1991) reported measured wetting and drying water saturation as a function of matric potentials, of tuff core samples from borehole USW H-1 located in Yucca Mountain, near the 366-m depth, and from outcrop material at Fran Ridge near Yucca Mountain, at temperatures to 70°C. Daily and Lin reported a high degree of variability among the samples, in measured water saturation at a given matric potential. They also concluded that lower water saturations were measured at the higher temperature. They

indicated that the hysteresis at room temperature was measurable, and that indirect evidence suggested a lack of measurable hysteresis at the higher temperature.

Roberts and Lin (1995 and 1996) reported moisture retention curves measured at temperatures to 93.6°C on samples from borehole USW-G4 in Yucca Mountain, at 349.6-m depth. They reported small hysteresis among the data at room temperature (p. 15 of Roberts and Lin, 1995) and observed a reverse in the hysteresis between the room-temperature data and the 94°C data (p. 5 of Roberts and Lin, 1996).

This report presents the moisture retention curves measured to 94°C on core samples of the Single-Heater Test (SHT) and Drift-Scale Test (DST). The SHT and the DST are two thermal tests conducted in the Exploratory Studies Facility in Yucca Mountain by the DOE. The description of the SHT can be found in Single Heater Test Status Report (CRWMS, 1997a). The description of the DST can be found in Drift Scale Test Design and Forecast Results (CRWMS, 1997b). The moisture retention curves of the SHT samples at room temperature were reported by Wilder (1997).

Matric Potential

The water suction potential of a porous medium is a sum of its matric potential and osmotic potential. This combined potential for retention of water can be estimated directly from the vapor pressure of the water in the material. This is because the vapor pressure of the water is lowered in a predictable way by interaction with the solid matrix and by solutes. If the water is relatively free of solutes (this is a good approximation for the pore water used in the tests), one may assume that the total water potential is primarily due to the matric potential.

The matric potential is the pressure potential that arises from the interaction of water with a solid matrix (Marshall and Holmes, 1992). Matric potential is defined by Kelvin's Law as

$$p = \rho R T \ln (e/e_0)/M \qquad (1)$$

where p is the matric potential in MPa, ρ is the density of water at the temperature of interest in g/cm^3, R is the universal gas constant (8.314 J/K·mol), T is temperature in K, e/e_0 is the relative humidity (RH), and M is the molecular weight of water (18.015 g/mole).

Equation (1) shows that matric potential is explicitly dependent on temperature. It is generally acknowledged that matric potential is also implicitly dependent on temperature because surface tension depends on temperature. The capillary pressure decreases with temperature for given water content because the surface tension in each capillary decreases with temperature.

Experimental Procedure

Sample Description and Preparation

The mineralogical compositions of the rock in the SHT and the DST regions are very similar. The major minerals in the rock are SiO_2 polymorphs (30.5 to 34.5%) and feldspars (65.4 to 67.1%). Minor minerals include zeolite, smectite and muscovite (Roberts and Viani, 1998). Samples from the SHT and the DST in the Exploratory Studies Facility (ESF), Yucca Mountain, Nevada, were prepared from cores taken from the boreholes. Tables 1 and 2 list the identification numbers, boreholes, depths, wet and dry densities, and porosities for the SHT and the DST samples respectively. Eleven SHT samples and 13 DST samples were prepared. The samples were subcored to a diameter of between 4.4 cm and 6.1 cm and cut into disks approximately 2.5 to 3.0 mm thick. Samples with obvious large cavities and inhomogeneous inclusions were avoided. The porosity of each sample was determined by subtracting the dry density from the saturated density and dividing by the water density. The average porosity for the DST samples is 10.0 ± 1.7%; for the SHT samples, it is 11.1 ± 1.1%.

Table 1. Single Heater Test samples prepared for moisture retention experiments.

Sample ID	Borehole	Depth (m)	Wet density (g/cm^3)	Dry density (g/cm^3)	Porosity
0047525.2	CHE-1	2.2	2.348	2.247	0.102
0047525.2A	CHE-1	2.3	2.350	2.249	0.102
0047526.2	CHE-1	4.6	2.349	2.240	0.109
0047527.2	CHE-1	8.2	2.345	2.246	0.0998
0047528.2	CHE-1	12.5	2.331	2.224	0.107
0047529.2	CHE-1	14.0	2.344	2.235	0.109
0047530.2A	CHE-2	14.8	2.294	2.167	0.127
0047531.2	CHE-2	5.0	2.332	2.222	0.111
0047533.2	CHE-2	12.7	2.290	2.156	0.135
0047534.2	CHE-2	15.2	2.331	2.229	0.103
0047535.2	CHE-2	17.6	2.314	2.195	0.119
Mean*		11 samples	2.33±0.02	2.22±0.03	0.111±0.011

*Statistical mean for 11 samples; errors represent one standard deviation for all samples collectively

Table 2. Drift Scale Test samples prepared for moisture retention experiments.

Sample ID	Borehole	Depth (m)	Wet density (g/cm^3)	Dry density (g/cm^3)	Porosity
01002163-1	CHE-1	92.3 –93.2	2.371	2.286	0.0853
01002176-1	CHE-2	128.9 –129.6	2.322	2.211	0.111
01002179-1	CHE-5	39.4 –40.1	2.386	2.303	0.0831
01002189-1	CHE-6	43.4 –44.1	2.307	2.216	0.0914
01002190-1	CHE-6	63.9 – 64.6	2.375	2.292	0.0835
01002194-1	CHE-6	99.7 –100.4	2.330	2.224	0.106

01002199-2	CHE-7	51.9 – 52.6	2.301	2.174	0.127
01002200-1	CHE-7	80.0 –80.7	2.363	2.273	0.0895
01002206-2	CHE-10	15.7 –16.3	2.329	2.227	0.102
01002207-2	CHE-10	27.3 –28.0	2.400	2.311	0.0891
01002209-2	CHE-10	75.6 –76.3	2.379	2.254	0.125
01002212-1	CHE-10	91.6 –92.3	2.368	2.243	0.124
01002215-1	CHE-10	124.0–124.7	2.361	2.282	0.0796
Mean*		13 samples	2.35±0.03	2.25±0.04	0.100±0.017

* Statistical mean for 13 samples; errors represent one standard deviation for all samples collectively

Measurement Procedures

The following procedure was used to perform the matric potential measurements. First, the samples were machined and the dimensions measured. The dry and saturated densities of the samples were then determined. These densities were used to calculate the porosity of the samples (See Tables 1 and 2). Next, the samples were placed in a vacuum oven at 35°C to reach a completely dry state. The samples were then placed in the relative humidity chamber at 25°C and 20% RH to start the measurement in the wetting cycle at room temperature. The sample weights were determined daily. A balance with a sensitivity of 0.01mg calibrated to a traceable standard was used to weigh the samples. When the weights reached a constant value for several days, it was assumed that equilibrium was established, and the sample weights were used to calculate the saturation level at that RH condition. Saturation is calculated by comparing the measured weights with dry weights and taking into account porosity. Then the RH was increased to 50%, and the procedures were repeated. This was repeated for the higher RH levels at 80 and 95%. After this, the RH was decreased according to the following steps: 80%, 50%, and 20% RH to start the measurements in the drying cycle at room temperature. The SHT samples at 25°C had additional measurements performed, during both wetting and drying, at 35% and 65% RH. The maximum saturation achieved at the highest RH (~98%) was between 30% and 40% (see below). The process was then repeated for the drying portion of the measurement. This cycle of measurement was repeated at different temperatures: 50°C and 94°C.

Measurement Uncertainty

The uncertainties involved in determining of the moisture retention curves include the measurements of weights, relative humidity, and sample size. The sample dimensions are used to determine sample wet and dry densities. It is estimated that the thickness of the sample can be determined to ± 0.01 mm and the diameter to ± 0.03 mm. For the samples used here, this results in an error in

sample volume of ~± 0.4%. The uncertainty in dry weight is estimated to be ~0.00002 g and for wet weight ~0.0001 g. The error in the wet weight is higher than that of the dry condition because of the difficulty in achieving and maintaining saturation levels of 100% at elevated temperature. These uncertainties result in errors in dry and wet densities of ~3%. When propagated through to porosity using methods outlined by Bevington and Robinson (1992), the error is ~1.0% porosity, or ~7-11% of the measurement.

When repetitive measurements, such as the determination of weights at a specified relative humidity, are made on samples over several days, the uncertainty in the measurement is often less than the statistical uncertainty in the mean of the measured parameter. In such cases, the error is taken as one standard deviation of the mean of the repeated measurements. The errors in saturation determined at specific temperature and RH vary from ~0.07 to 0.4%. Thus, the relative uncertainty is between ~1% and 10%, with a 1% to 2% error most common.

The uncertainty in the relative humidity is approximately ± 2% RH. When propagated through Equation (1) to matric potential, the absolute uncertainties are fairly low, but the relative uncertainties are high at the matric potentials closest to zero.

The temperatures reported are the mean temperatures recorded during the time periods of the measurements. The highest statistical uncertainty (one standard deviation) is about ±0.6°C, but is generally less than ±0.3°C.

Results and Discussion

SHT Samples

The samples of the SHT used in the moisture retention curve measurements are listed in Table 1. Moisture retention curves of the SHT samples at temperatures of 25.1°C, 49.6°C, and 93.7°C are shown in Figures 1 to 3 respectively. Only the "average" properties are shown for clarity. The averages are the mean saturation and matric potential of all samples. The error bars for saturation are the standard deviation from the average saturation at a matric potential level of all samples. There is very little hysteresis at all temperatures. There is virtually no change between the data at 25°C and 50°C. As expected, the moisture retention at 94°C is less than that at the lower temperatures. Figure 4 shows the moisture retention curves of the SHT samples at 25°C after the samples had gone through the temperature cycle. The temperature cycle has a very small effect on the moisture retention: the post-temperature-cycle data show a slightly smaller moisture retention than the first room-temperature data.

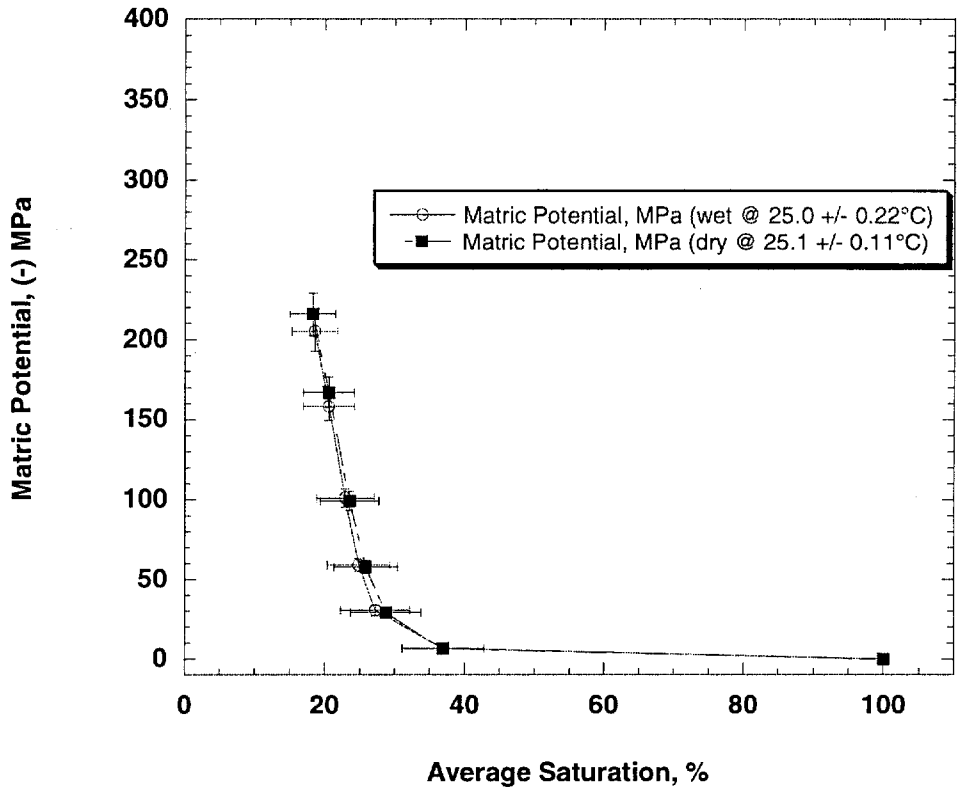

Figure 1. Matric potential versus average saturation for 11 SHT samples at 25.1°C. Lines connect the points and do not represent curve fits. Open circles and solid line represent the wetting curve. Solid squares and dashed line represent the drying curve. The point at 100% saturation is inferred.

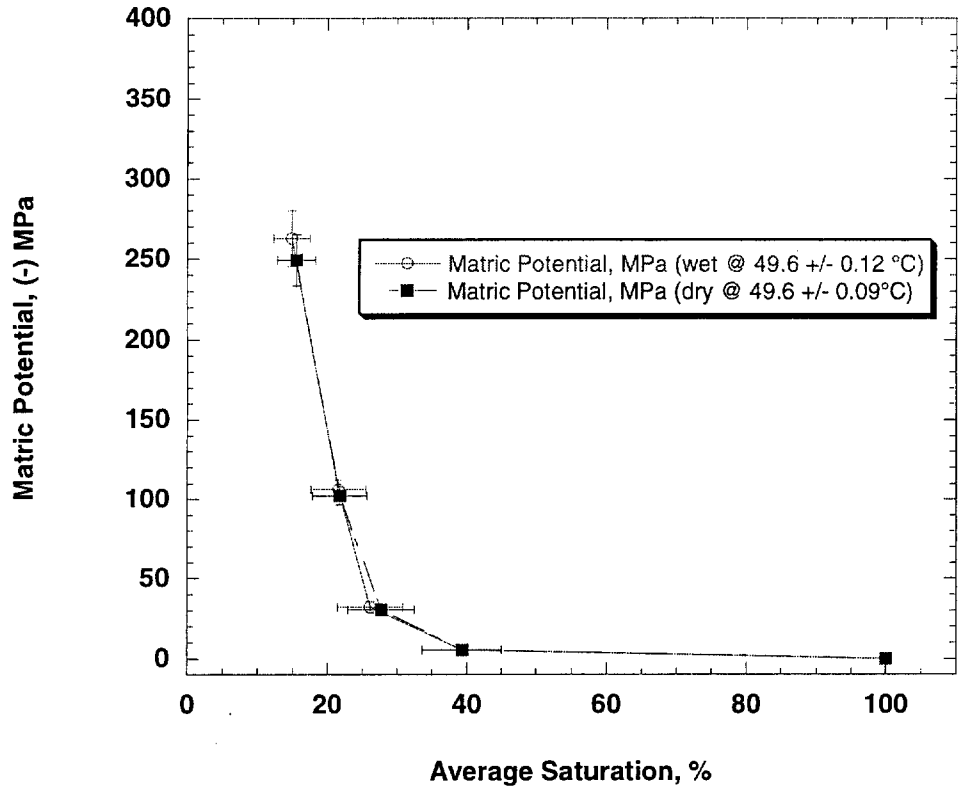

Figure 2. Matric potential versus average saturation for 11 SHT samples at 49.6°C. Lines connect the points and do not represent curve fits. Open circles and solid line represent the wetting curve. Solid squares and dashed line represent the drying curve. The point at 100% saturation is inferred.

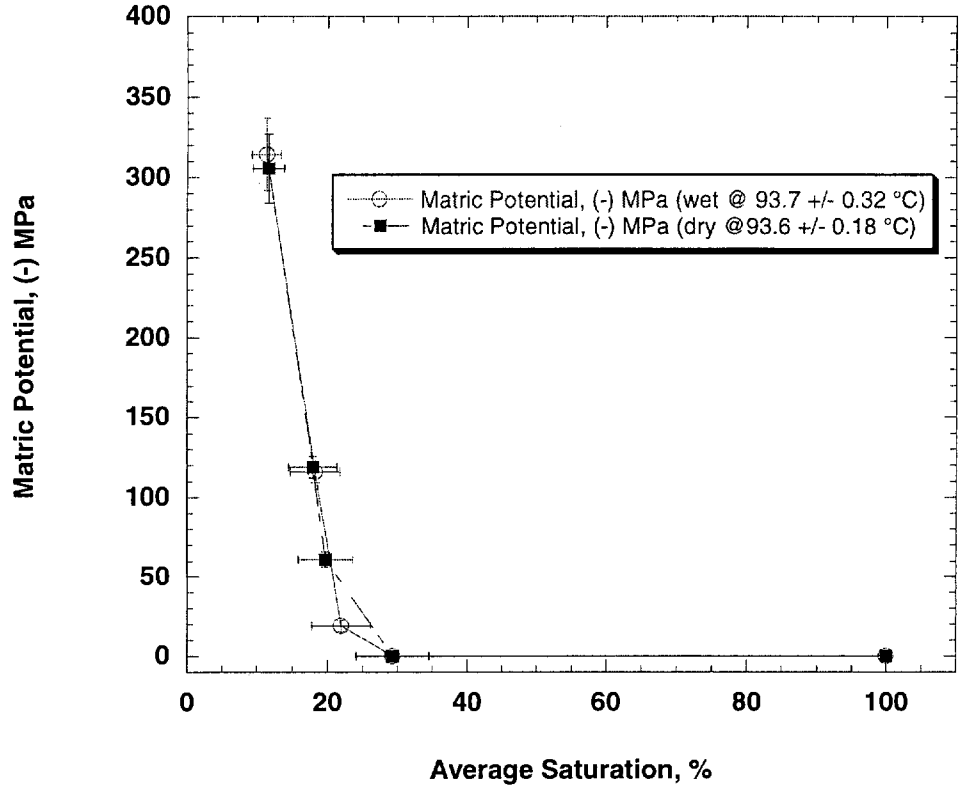

Figure 3. Matric potential versus average saturation for 11 SHT samples at 93.7°C. Lines connect the points and do not represent curve fits. Open circles and solid line represent the wetting curve. Solid squares and dashed line represent the drying curve. The point at 100% saturation is inferred.

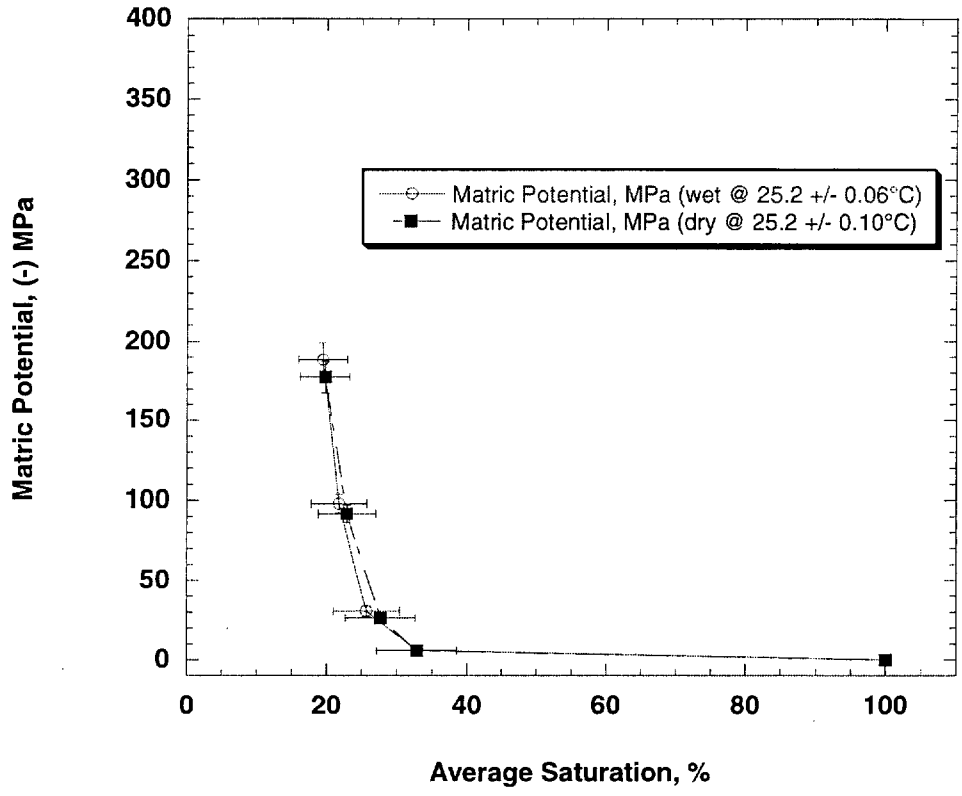

Figure 4. Matric potential versus average saturation for 11 SHT samples at 25.2°C after the temperature cycle. Lines connect the points and do not represent curve fits. Open circles and solid line represent the wetting curve. Solid squares and dashed line represent the drying curve. The point at 100% saturation is inferred.

DST Samples

The samples of the DST used in the moisture retention curve measurements are listed in Table 2. Moisture retention curves of the DST samples at temperatures of 25.1°C, 49.6°C, and 93.7°C are shown in Figures 5 to 7 respectively. Only the "average" properties are shown for clarity. The averages are the mean saturation and matric potential of all samples. The error bars for saturation are the standard deviation from the average saturation at a matric potential level of all samples. Similar to the SHT data, there is very little hysteresis observed between the wetting and drying curves at all temperatures. Previous measurements on similar rock showed significant hysteresis under certain conditions (Daily and Lin, 1991). There is also very little difference between the 25.1 and 49.6°C curves. The data at 93.7°C show lower moisture retention than the lower temperature data. For comparison, samples from USW-G4 showed a significant temperature dependence of moisture retention on temperature (Roberts and Lin, 1995 and 1996). Figure 8 shows the moisture retention data at 25°C after the temperature cycle. The temperature cycle has a very small effect on the moisture retention: the post-temperature-cycle room-temperature data show a slightly smaller moisture retention than the initial room-temperature data.

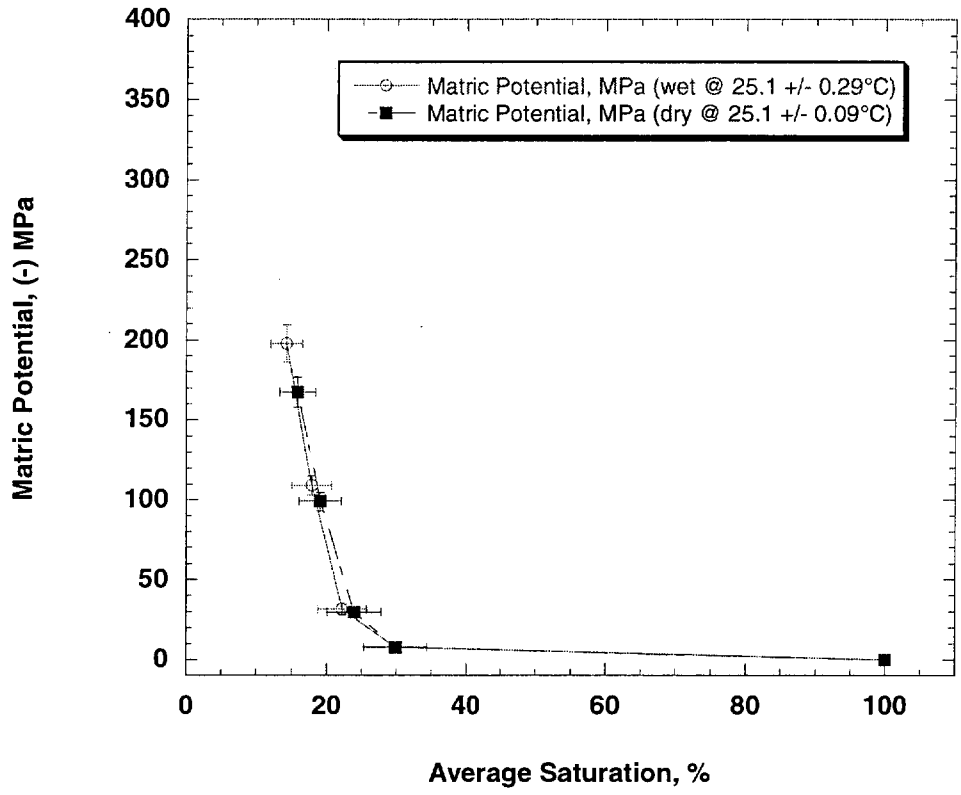

Figure 5. Matric potential versus average saturation for 13 DST samples at 25.1°C. Lines connect the points and do not represent curve fits. Open circles and solid line represent the wetting curve. Solid squares and dashed line represent the drying curve. The point at 100% saturation is inferred.

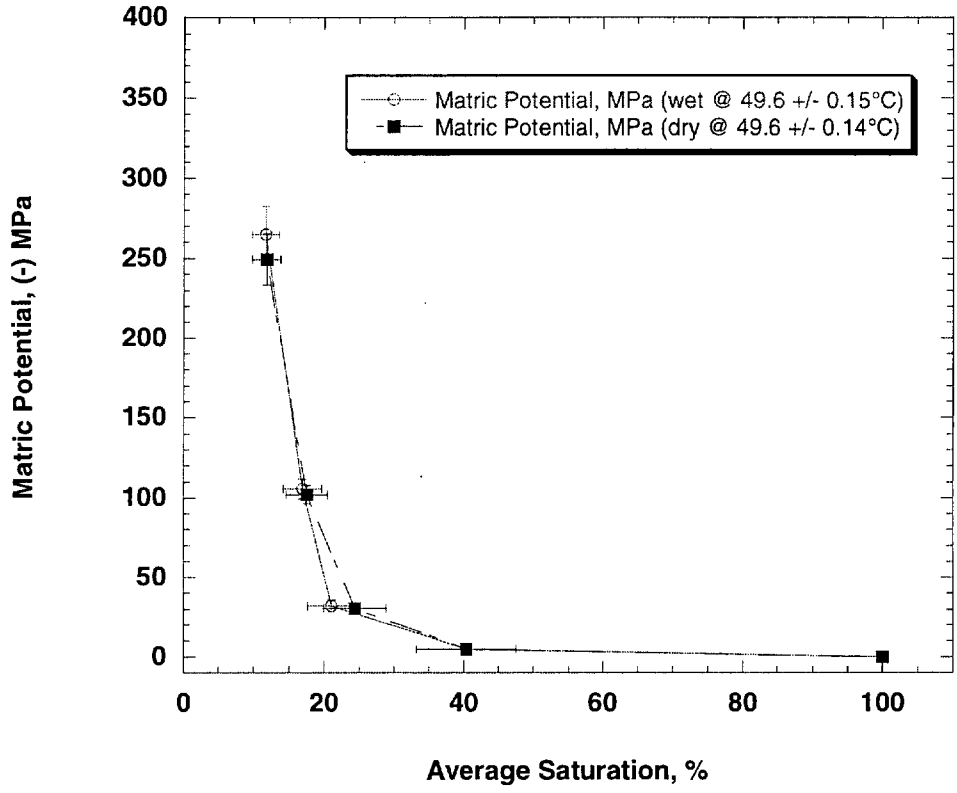

Figure 6. Matric potential versus average saturation for 13 DST samples at 49.6°C. Lines connect the points and do not represent curve fits. Open circles and solid line represent the wetting curve. Solid squares and dashed line represent the drying curve. The point at 100% saturation is inferred.

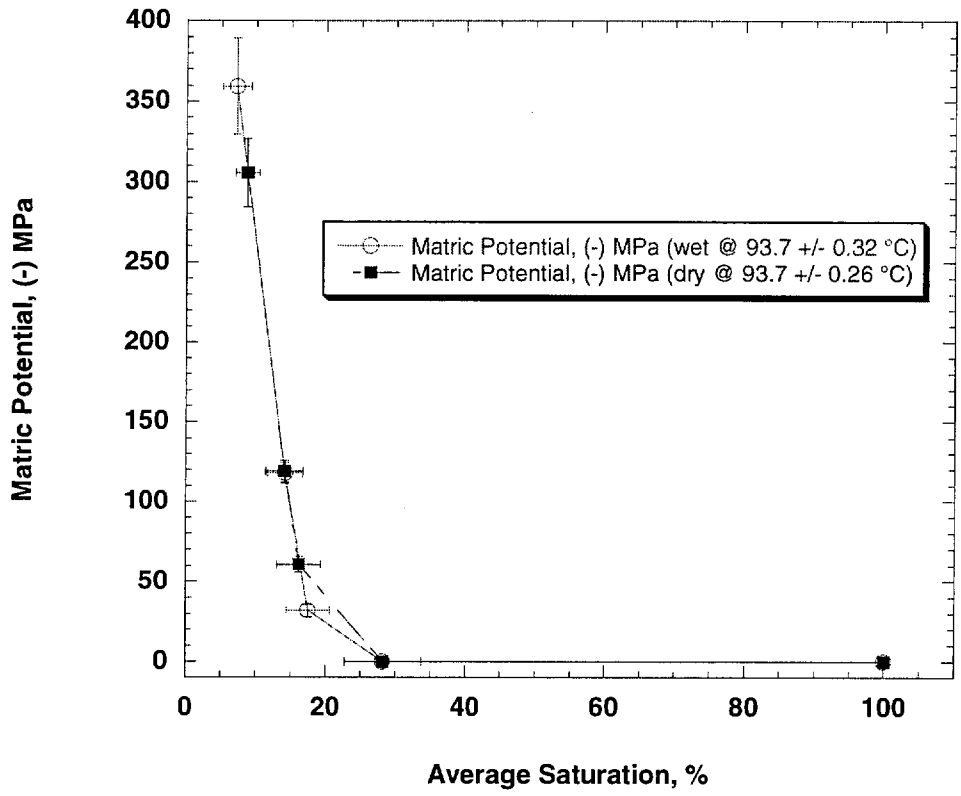

Figure 7. Matric potential versus average saturation for 13 DST samples at 93.7°C. Lines connect the points and do not represent curve fits. Open circles and solid line represent the wetting curve. Solid squares and dashed line represent the drying curve. The point at 100% saturation is inferred.

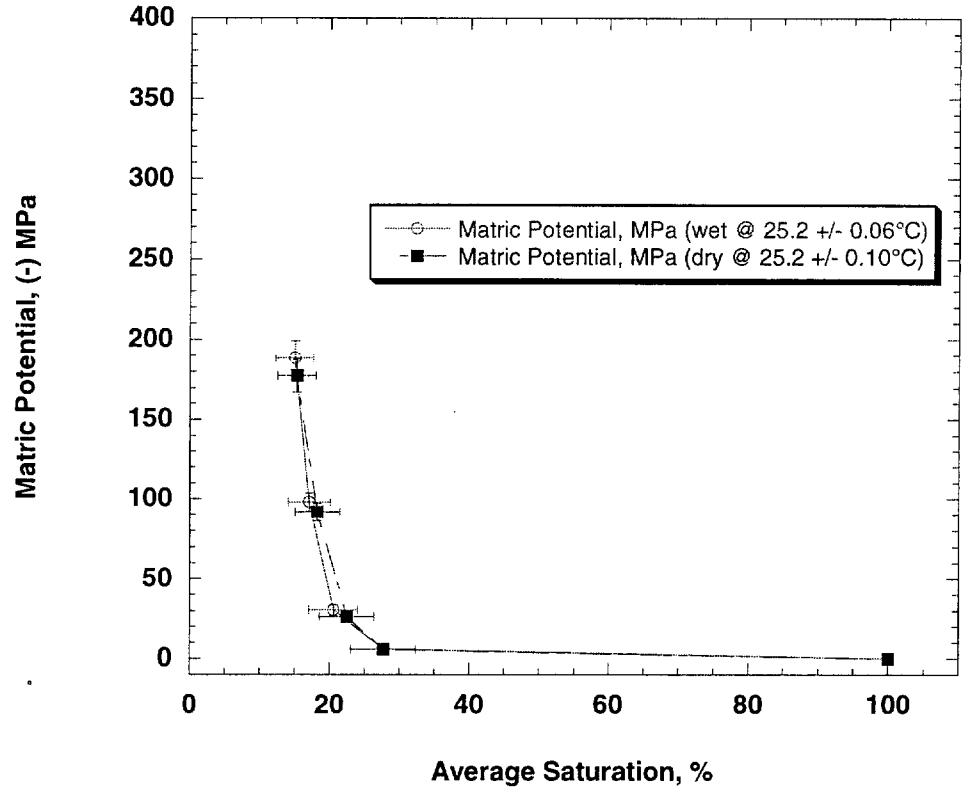

Figure 8 Matric potential versus average saturation for 13 DST samples at 25.2°C after the temperature cycle. Lines connect the points and do not represent curve fits. Open circles and solid line represent the wetting curve. Solid squares and dashed line represent the drying curve. The point at 100% saturation is inferred.

Summary

The moisture retention curves are dependent on temperature. The effect is not significant between 25°C and 50°C but seems to be significant between 50°C and 94°C. The temperature effect on the moisture retention curves is always to decrease the level of saturation at a matric potential level with increasing temperature. This observation holds for both the DST and the SHT samples. The SHT samples show greater moisture retention than the DST samples at all temperatures. The difference decreases slightly with increasing temperature. The maximum saturation that can be reached in those samples depends on temperature. At 25.1°C the maximum saturation achieved is about 30% for the DST samples and about 36% for the SHT samples. At 49.6°C this increases to about 40% for the DST samples and about 39% for the SHT samples, but at 93.7°C it decreases to about 28% for the DST samples and about 29% for the SHT samples. The data of the SHT samples show greater moisture retention than that of the USW H-1, USW G-4, and Fran Ridge samples. The data of the DST samples show greater moisture retention than that of USW G-4 and the Fran Ridge samples. The data of the DST samples are at the high end of the results of the USW H-1 samples. The data of both SHT and DST samples are at the lower bound of that shown by Flint (1998).

Acknowledgments

The authors thank Gina Kaiper for editing this manuscript. This work was supported by the Yucca Mountain Site Characterization Project. Work performed under the auspices of the US. Department of Energy by the University of California, Lawrence Livermore National Laboratory, under Contract W-7405-Eng-48.

References

Bevington, P.R., and D K. Robinson, (1992) *Data Reduction and Error Analysis for the Physical Sciences*, 2nd ed., San Francisco, CA: McGraw-Hill, 328 pp.

CRWMS, (1997a) *Single Heater Test Status Report*, Civilian Radioactive Waste Management System Management & Operation Contractor report, BAB000000-01717-5700-00002 Rev 00, TRW Environmental Safety Systems Inc., Las Vegas, NV 89134.

CRWMS, (1997b) *Drift Scale Test Design and Forecast Results*, Civilian Radioactive Waste Management System Management & Operation Contractor report, BAB000000-01717-4600-00007 Rev 00, TRW Environmental Safety Systems Inc., Las Vegas, NV 89134.

Daily, W., and W. Lin, (1991) "Laboratory Determined Suction Potential of Topopah Spring Tuff at High Temperatures," in *Proceedings of the Second Annual International Conference on High Level Radioactive*

Waste Management, Las Vegas, NV, April 28-May 3, 1991, American Nuclear Society, La Grange Park, IL, pp. 583-588.

Flint, L.E., (1998) *Characterization of Hydrogeologic Units Matrix Properties, Yucca Mountain, Nevada*, Water Resources Investigations Report, 97-4243, U.S. Geological Survey, Denver, CO.

Klavetter, E.A., and R.R. Peters, (1987) *An Evaluation of the Use of Mercury Porosimetry in Calculating Hydrologic Properties of Tuff from Yucca Mountain, Nevada*, SAND86-0286-UC-70, Sandia National Laboratories, Albuquerque, NM.

Marshall, T.J., and J.W. Holmes, (1992) *Soil Physics*, 2nd ed., Cambridge, U.K.: Cambridge University Press, 374 pp.

Peters, R.R.; E.A. Klavetter; I.J. Hall; S.C. Blair; P.R. Heller; and G.W. Gee, (1984) *Fracture and Matrix Hydrologic Characteristics of Tuffaceous Materials from Yucca Mountain, Nye County, Nevada*, SAND84-1471, Sandia National Laboratories, Albuquerque, NM.

Roberts, J.J., and W. Lin, (1995) *Hydrological Property Measurements of Topopah Spring Tuff*, Report, Lawrence Livermore National Laboratory UCRL-ID-119033, Livermore, CA.

Roberts, J.J., and W. Lin, (1996) *Report on Laboratory Tests of Drying and Re-Wetting of Intact Rocks*, Report, Lawrence Livermore National Laboratory UCRL-ID-121513, Livermore, CA.

Roberts, S., and B. Viani, (1998) *Determination of Mineral Abundances in Samples from the Exploratory Studies Facility, Yucca Mountain, Nevada, Using X-ray Diffraction*, Lawrence Livermore National Laboratory report UCRL-ID-129748, Livermore, CA.

Wilder, D. G., (1997) *Near-Field and Altered-Zone Environment Report, Volume I: Technical Bases for EBS Design, Rev. 1*, Lawrence Livermore National Laboratory Report UCRL-LR-124998, Vol. I, Livermore, CA.